Experimental study on the consolidation of saturated silty clay subjected to cyclic thermal loading

Bing Bai[*] and Xiaoying Shi

School of Civil Engineering, Beijing Jiaotong University, Beijing, 100044, P.R. China

Abstract. The objective of this paper is to experimentally study the consolidation of saturated silty clay subjected to repeated heating-cooling cycles using a modified temperature-controlled triaxial apparatus. Focus is placed on the influence of the water content, confining pressure, and magnitudes and number of thermal loading cycles. The experimental results show that the thermally induced pore pressure increases with increasing water content and magnitude of thermal loading in undrained conditions. After isothermal consolidation at an elevated temperature, the pore pressure continues to decrease and gradually falls below zero during undrained cooling, and the maximum negative pore pressure increases as the water content decreases or the magnitude of thermal loading increases. During isothermal consolidation at ambient temperature after one heating-cooling cycle, the pore pressure begins to rise due to water absorption and finally stabilizes at approximately zero. As the number of thermal loading cycles increases, the thermally induced pore pressure shows a degrading trend, which seems to be more apparent under a higher confining pressure. Overall, the specimens tested show an obvious volume reduction at the completion of a series of heating-cooling cycles, indicating a notable irreversible thermal consolidation deformation.

Keywords: silty clay; magnitudes of thermal loading; isothermal consolidation; pore pressure; water content

1. Introduction

Studies on the thermo-hydro-mechanical behaviors of saturated soils are important for a number of engineering applications, including the storage of hot fluids, the extraction of geothermal energy, the isolation of nuclear waste, road subgrading and the construction of waste containment facilities (Towhata *et al.* 1993, Abuel-Naga *et al.* 2009, Delage *et al.* 2010).

Previous researches on the consolidation and shear strength of saturated soils were mainly concerned with the long-term deformation properties (Le *et al.* 2015), cyclic effects (Cheng and Wang 2016) under mechanical loading, etc. In recent years, much effort has been invested in experimentally studying the thermal properties of soils. Hueckel and Baldi (1990) designed a temperature-controlled triaxial apparatus to study the thermoplasticity of saturated clays in the temperature range of 18°C and 115°C. Using an isotropic compression cell, Delage *et al.* (2012) conducted an experiment with Boom clay to investigate the thermal volume change of the clay-water system, thermal consolidation, and changes of permeability with temperature. More recently,

---

∗Corresponding author, Professor, E-mail: baibing66@263.net

a new temperature-controlled triaxial apparatus was developed by combining a conventional pressure chamber with an electric thermostat-box. The experimental results revealed that temperature had a certain influence on thermal volume change, soil-water characteristic curves and shear strength (Bai *et al*. 2014). A new hollow cylinder triaxial cell was designed to study the thermo-hydro-mechanical behaviors of low-permeability argillites. The main advantage of this apparatus is the addition of lateral hydraulic connections placed on the inner and outer walls of the hollow cylinder sample to reduce the drainage length (Monfared *et al*. 2011). A comprehensive laboratory study on the mechanical behaviors of a Kaolin clay discussed the thermal effects on the volume change during drained heating, the preconsolidation pressure and compressibility index, and the shear strength and critical state (Cekerevac and Laloui 2004). The thermally induced volume change of normally consolidated or overconsolidated saturated soft Bangkok clay measured by a modified oedometer test was predicted by a thermal elastic-plastic model (Abuel-Naga *et al*. 2007). In addition, Villar *et al*. (2010) experimentally investigated the dependence of the swelling strains of bentonite on the temperature, permeability of water saturated bentonite with temperature, and water retention curves of bentonite compacted at different dry densities. Previous studies suggested that temperature had a veritable impact on the consolidation behaviors of the underthrust sediments, with increasing temperature leading to an enhanced pore space reduction (Hüpers and Kopf 2009). An impact was also found on particle size, water content, specific gravity, plasticity, activity index, swelling and compression index, and strength properties of kaolinite and bentonite (Yilmaz 2011). A theoretical framework suggested that the thermal pressurization phenomenon of the fluid-saturated porous materials under an undrained condition was controlled by the discrepancy between the thermal expansion of the pore fluid and that of the solid phase, the stress-dependency of the compressibility and the non-elastic volume changes of the porous materials (Ghabezloo and Sulem 2010).

Research interest in the thermal responses of porous materials to heating-cooling processes has grown in recent years because they can be utilized to interpret a series of physical phenomena and problems. Some scholars have experimentally investigated the effect of thermal loading paths (Cekerevac and Laloui 2004), heating history (Abuel-Naga *et al*. 2007, Burghignoli *et al*. 2000), reversibility of thermal consolidation (Cui *et al*. 2000, Graham *et al*. 2001), and natural or artificial temperature fluctuations (Francois *et al*. 2009, Yavuzturk *et al*. 2005). For example, Sultan *et al*. (2002) and Abuel-Naga *et al*. (2007) analyzed the thermal volume changes of Boom clay and soft Bangkok clay under a single drained heating-cooling process at different OCR values (e.g., OCR = 1, 2, 4, 8). Both studies showed that thermally induced consolidation was not fully reversible when the temperature returns to its initial value (see also Baldi *et al*. 1988, Graham *et al*. 2001), and the extent of reversibility appeared to differ significantly from soil to soil. Blond *et al*. (2003) established a theoretical pressure diffusion equation that governed the fluctuation of the interstitial pressure and developed a closed-form solution of the maximum fluid pressure and its location of a porothermoelastic half-space submitted to cyclic thermal loading. Bai (2006) derived an analytical method for the fluctuation responses of saturated porous media to cyclic thermal loading using the Laplace transform and the Gauss-Legendre method of Laplace transform inversion. Cui *et al*. (2005) conducted a field simulation of in situ water content and temperature changes due to seasonal ground-atmospheric interactions. Bai and Chen (2011) discussed the degradation effect of saturated clay subjected to cyclic thermal loading using a temperature-controlled triaxial apparatus.

However, the thermal behaviors of porous materials in response to cyclic temperature changes are not yet completely understood in the existent literature, thereby necessitating more experimental studies. We therefore conducted an experiment to study the consolidation of

saturated silty clay subjected to repeated heating-cooling cycles using a modified temperature-controlled triaxial apparatus. Focus is placed on the influence of the water content, confining pressure, and magnitudes and number of thermal loading cycles. We analyzed the evolutionary processes of the thermal consolidation during the repeated heating-cooling cycle, and we discuss the degradation and reversibility behaviors of the thermally induced pore pressures and consolidation volumetric strains with cycles.

2. Materials, equipment, and experimental scheme

2.1 Sample preparation

The consolidation tests were performed on silty clay. To obtain uniform samples, air-dried sediments were ground to soil fines that could pass through a 0.5-mm sieve. The liquid limit was $LL = 31.4\%$, plastic limit $PL = 17.6\%$, plasticity index $PI = 13.8$, and specific gravity of the soil solids $G_s = 2.71$. The grain size distribution revealed that approximately 81.2% by weight was smaller than 0.075 mm. The mineralogical content of the materials obtained from X-ray diffraction analysis yielded 45.7% kaolinite, 43.1% quartz, 7.8% chlorite, and 3.4% illite. The sieved soils were mixed to an initial water content of approximately 19.7%-23.7% and were kept in a plastic container for at least 24 hours. The soil specimens, which were 3.91 cm in diameter and 8 cm in height, were prepared with a cylindrical specimen mold. Then, the mold, together with the soil specimens, was transferred to a large vessel for saturation by applying a vacuum pump for at least 6 hours and allowing the de-aired water to flow through the specimens. The degree of saturation S_r was determined to be more than 96.9%. In all tests, vertical strips of filter paper were attached to the sides of the specimens to speed up the consolidation process. In addition, filter paper disks were placed on both ends of the specimens to prevent the intrusion of soil fines into the pores of the porous stones. Prior to placement of the filter paper, the porous stones were boiled in distilled water until they reached a desirable saturation.

2.2 Equipment

The consolidation tests were performed using a triaxial shear device especially modified for variable thermal loading, a schematic diagram of which is shown in Fig. 1. The device can measure thermally induced consolidation deformation at a primary temperature and axial shear strength (Bai *et al*. 2014). The temperature inside the pressure chamber can vary from 20°C to 100°C. The temperature of the soil specimen is increased indirectly by heating the water in the pressure chamber. The thermal loadings of different magnitudes or paths are applied by an electro-thermal plate installed inside the hollow metallic sleeve of the chamber and connected to a thermocouple in the cell (to avoid specimen disturbance), and asbestos outside the electro-thermal plate filled within the hollow metallic sleeve is used to isolate the pressure chamber. The sensitivity of the thermo-control system is ±0.1°C. Pore pressure is measured with an electronic pore pressure transducer (measuring range: 0−1 MPa) attached to the center of the specimen base and connected to a digital monitoring apparatus. The confining pressure is measured with another pressure transducer (measuring range: 0−1 MPa) attached to the bottom of the pressure chamber. The pressure measurements are resolved to 0.1 kPa.

The apparatus had been appropriately calibrated for temperature variations. As shown in Fig. 1, the drainage line (a spiral stainless steel tube) was immersed in a cooling bath at a constant
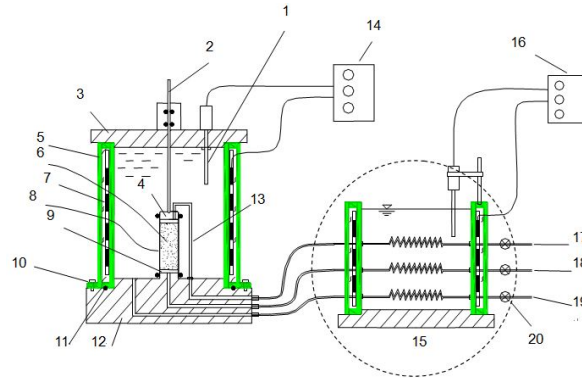
Note: 1, thermocouple; 2, axial load piston; 3, upper plate; 4, top cap; 5, metallic sleeve; 6, specimen; 7, cylindrical electro-
thermal plate; 8, membrane; 9, porous stone; 10, fastening bolt; 11, O-rings; 12, pedestal; 13, metallic drainage tube;
14, thermo-control system; 15, cooling bath; 16, temperature regulator; 17, outflow pore water measurement system;
18, pore pressure measurement system; 19, confining pressure generator; 20, on-off valve

Fig. 1 Test apparatus for thermal consolidation

temperature of 25°C to guarantee that the volumes of water expelled from the soil specimens would be measured at the same temperature. As a result, the volumetric strains are comparable.

2.3 Experimental scheme

The soil specimens were subjected to different effective confining pressures ($\sigma_3' = 50, 100, 150$ kPa) at an ambient temperature of 25°C, and the drainage valve located at the top cap was then opened to allow the pore pressure to dissipate. The volume of water expelled from the soil specimens was measured with a burette in the drain valve, serving as the index of volume change, from which the volumetric strain could be calculated. The specimens were then subjected to six repeated cycles of heating and cooling (25°C $\rightarrow$ 75°C $\rightarrow$ 25°C $\rightarrow$ 75°C…) under a constant confining pressure, during which drainage was not permitted. When it reached a given temperature (e.g., $T = 75$°C) or dropped to the initial temperature (i.e., $T_0 = 25$°C), the drainage valve was opened to allow dissipation or absorption. The magnitude of thermal loading was expressed as $\theta = T - T_0$, where T and T_0 were the current and initial temperature, respectively. Because the low-plasticity specimens in this study exhibited a low water-swelling effect, the expansion or shrinkage of the specimens is mainly attributed to temperature variations. A summary of the experimental scheme is given in Table 1 in which we primarily considered the influences of the water content w, confining pressure σ_3', magnitude of thermal loading θ and number of thermal loading cycles N.

3. Isothermal consolidation processes

The specimens underwent isothermal consolidation at a primary temperature T_0 (i.e., 25°C) under different effective confining pressures, and the resulting normalized pore pressure u/σ_3' and consolidation volumetric strain ε_v are plotted against time t in Fig. 2. In the early periods of consolidation, the pore pressure drops rapidly, as shown in Fig. 2(a), which renders an obvious consolidation volumetric strain, as shown in Fig. 2(b). After approximately $t = 300$ min, the pore pressure is dissipated to nearly zero, and correspondingly, a steady consolidation volumetric strain

Table 1 Experimental scheme

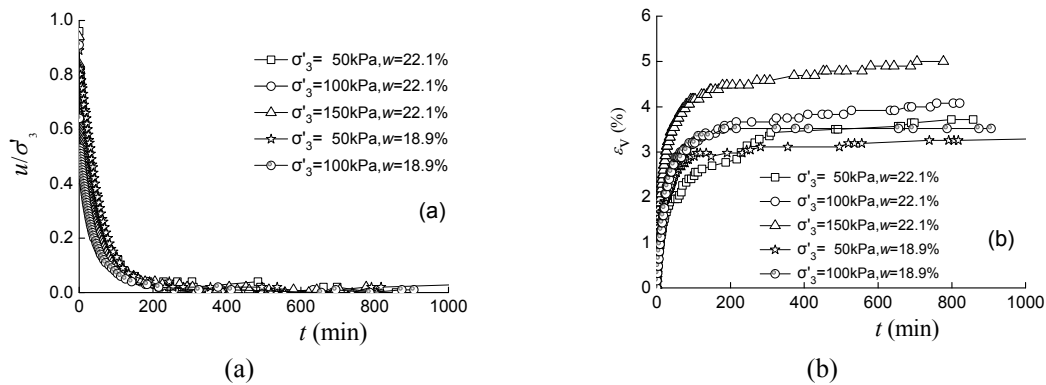| Number	Water content w (%)	Dry unit weight γ_d (kN/m³)	Degree of saturation S_r	Confining pressure σ_3' (kPa)	Primary temperature T_0 (°C)	Elevated temperature T (°C)
1	22.1	16.5	97.8	50	25	75
2	22.1	16.5	97.8	100	25	75
3	22.1	16.5	97.8	150	25	75
4	18.9	17.3	97.1	50	25	75
5	18.9	17.3	97.1	100	25	75
6	25.1	15.5	96.9	50	25	75
7	25.1	15.5	96.9	50	25	50

Fig. 2 Consolidation process under isothermal condition: (a) pore pressure; and (b) volumetric strain

is observed. Test results show that the higher the confining pressure, the greater the consolidation deformation. For instance, when $w = 22.1\%$, the consolidation deformation is 3.7%, 4.0%, and 4.9% for $\sigma_3' = 50$, 100, and 150 kPa, respectively, as shown in Fig. 2(b).

Fig. 2 also shows the effects of water content on consolidation. In general, the consolidation volumetric strain increases as the water content increases. For instance, when $\sigma_3' = 100$ kPa, the drained volumetric strain tends to stabilize at approximately $\varepsilon_v = 3.5\%$ for $w = 18.9\%$ and $\varepsilon_v = 4.0\%$ for $w = 22.1\%$.

4. Temperature variations

The temperature evolution inside the specimen is very complex during heating or cooling under undrained conditions, and in general lags behind that of the cell (Abuel-Naga *et al.* 2007). Therefore, the temperature inside the pressure chamber is taken as the temperature of the specimen in this study, and measured in the steady state of heating or cooling. Fig. 3 shows the temperature evolutions of specimens with $w = 22.1\%$ during the heating-cooling cycles. It shows that during undrained heating, the temperature rises rapidly until it reaches the given value. The temperature then fluctuates between 74.5°C and 75.5°C, which can be attributed to the heat dispersion of the
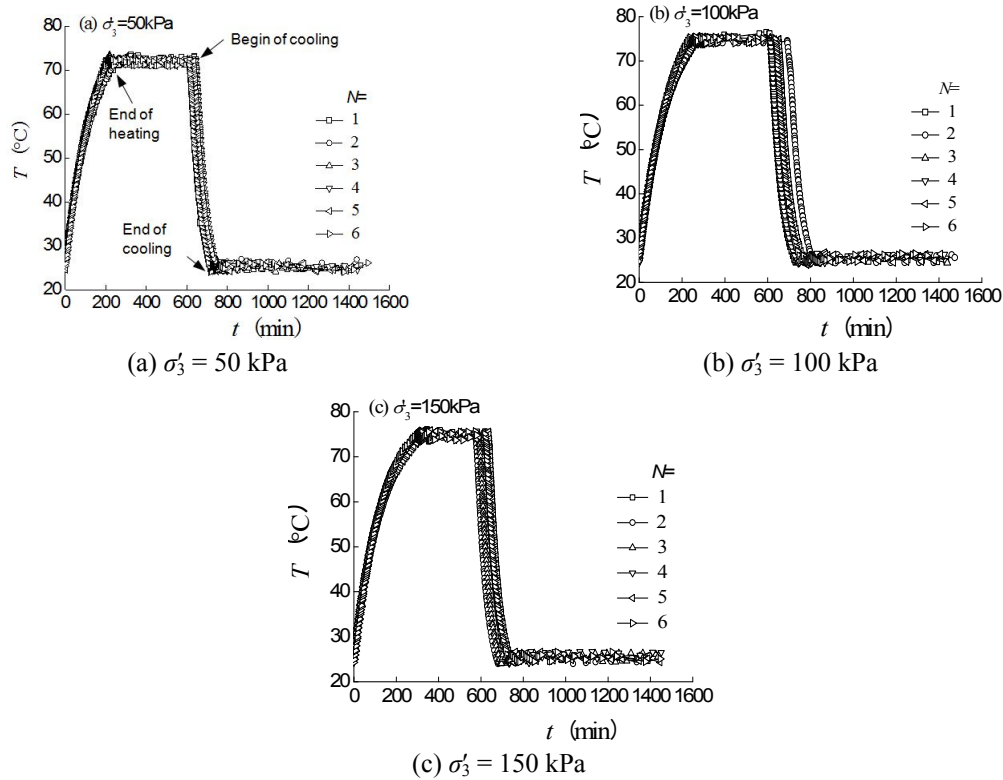
(a) $\sigma_3' = 50$ kPa

(b) $\sigma_3' = 100$ kPa

(c) $\sigma_3' = 150$ kPa

Fig. 3 Temperature variations during repeated heating-cooling processes ($w = 22.1\%$, $\theta = 50°C$)

apparatus and the inflow of low-temperature water to compensate for the outflow of pore water caused by consolidation. The temperature fluctuation in this study is generally within the permissible range of the thermal consolidation test. During undrained cooling, the temperature drops at a gradually decreasing rate because the temperature difference between the pressure chamber and laboratory room is gradually reduced with time. In addition, Fig. 3 shows that the temperature variation is almost independent of the magnitudes of confining pressures or the number of thermal loading cycles during the repeated heating-cooling cycles.

5. Pore pressure variations

5.1 Pore pressure variations over time

Fig. 4 shows the pore pressure evolutions of the specimens with $w = 22.1\%$ during the heating-cooling cycles. During undrained heating, the pore pressure rises rapidly in response to the rapidly increasing temperature, and then it reaches a maximum value. During isothermal consolidation at 75°C, the pore pressure declines continuously to a steady value of nearly zero in a short time. A noteworthy phenomenon is that the maximum normalized pore pressures appear to have a decreasing tendency with the increase of confining pressures. For example, when $N = 1$, the maximum normalized pore pressures are 1.0, 0.97, and 0.85 for $\sigma_3' = 50$, 100, and 150 kPa, respectively. During undrained cooling, the pore pressure falls below zero and gradually continues
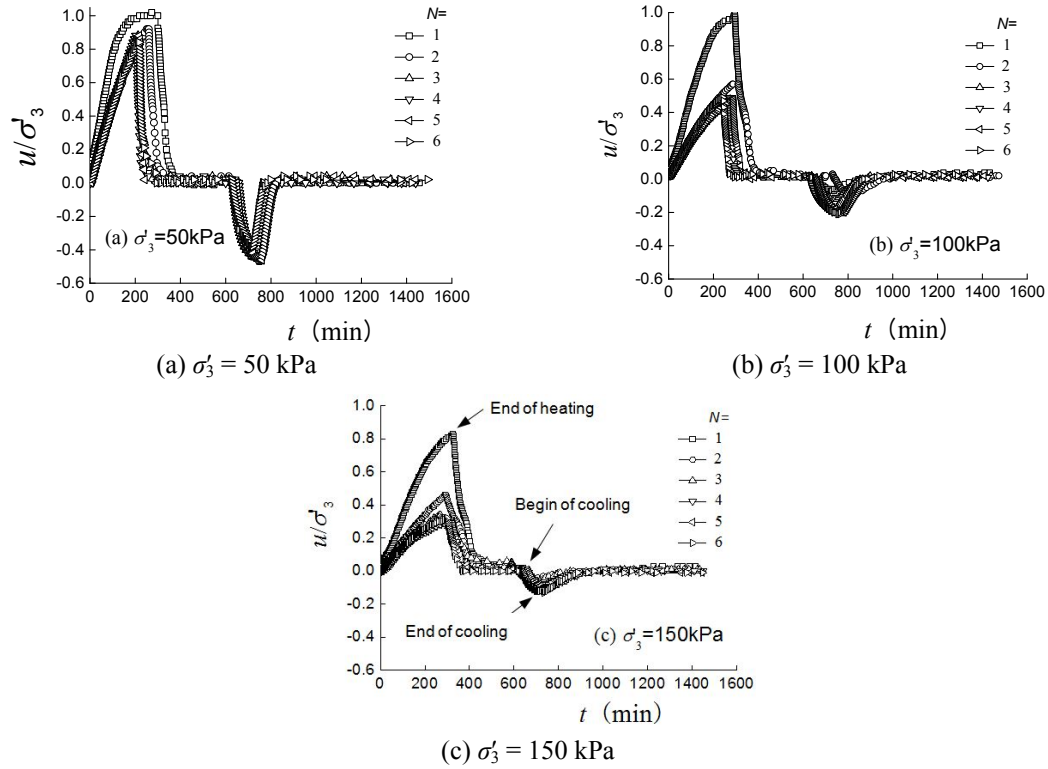
(a) $\sigma_3' = 50$ kPa

(b) $\sigma_3' = 100$ kPa

(c) $\sigma_3' = 150$ kPa

Fig. 4 Pore pressure variations during repeated heating-cooling processes ($w = 22.1\%$, $\theta = 50°C$)

to decrease, e.g., $u/\sigma_3' = -0.43$ when $\sigma_3' = 50$ kPa and $N = 1$. The negative pore pressure is due to the solid grains differing from the pore water in the thermal expansion coefficients, with the former having a smaller shrinkage deformation than the latter. However, during isothermal consolidation at 25°C, the pore pressure begins to rise as the result of water absorption due to the negative pore pressure, finally stabilizing at approximately zero. As the time for the pore pressure to be fully dissipated during the isothermal consolidation at 75°C (or 25°C) differs in different temperature cycles, the time intervals for different periods also differ slightly, ranging from 1400 min to 1500 min.

Although the plots of pore pressures against time are largely similar for different numbers of thermal loading cycles or magnitudes of confining pressures, a particularly noteworthy phenomenon is that with the increase of the cyclic number, the thermally induced pore pressure shows a degrading trend. Actually, the factors such as the level of confining pressure, the magnitude and number of cyclic thermal loading are always coupled together. It seems to be more apparent under higher confining pressures, because in such circumstances the specimens tend to be more obvious over-consolidated state due to the greater thermal consolidation deformation in the former heating-cooling cycles. More specifically, every time the specimens are heated to the given temperature (i.e., 75°C), the maximum normalized pore pressure will decrease slightly. For example, when $\sigma_3' = 50$ kPa, the maximum normalized pore pressure is 1.0, 0.9, and 0.87 for $N = 1$, 2, and 3, and approximately 0.85 for $N = 4$, 5, and 6, respectively; and every time the temperature returns to the initial value under the undrained condition, the minimum normalized pore pressure

will decrease slightly. For example, when $\sigma_3' = 50$ kPa, the minimum normalized pore pressure is −0.43, −0.48 and −0.50 for $N = 1$, 2, and 3 and approximately −0.52 for $N = 4$, 5, and 6, respectively. Actually, the specimens will show an over-consolidated state with increasing temperature cycles and will gradually take on a reversible state from an irreversible process of thermodynamics.

5.2 Effects of water content on pore pressure

Fig. 5 shows the effects of water content ($w = 18.9\%$ and 22.1%) on pore pressures when a constant confining pressure of 100 kPa is applied. During undrained heating, the thermally induced pore pressure rises at a comparable rate, but the maximum normalized pore pressure is slightly higher when $w = 22.1\%$; for example, when $N = 1$, it is 0.84 and 0.98 for $w = 18.9\%$ and 22.1%, respectively. Correspondingly, the minimum pore pressure is lower when $w = 18.9\%$; for example, when $N = 1$, it is −0.24 and −0.11 for $w = 18.9\%$ and 22.1%, respectively. However, the difference regarding pore pressure as the function of water content is most evident for the first two cycles and then vanishes gradually with the increase of the number of thermal loading cycles.

5.3 Effects of magnitude of thermal loading on pore pressure

Fig. 6 shows the effects of the magnitude of thermal loading on pore pressures when $\sigma_3' = 50$ kPa and $w = 25.1\%$. During undrained heating, the pore pressure rises in a similar way for $\theta = 25°C$ and $\theta = 50°C$, but the maximum normalized pore pressure is dramatically increased when $\theta = 50°C$. For example, when $N = 1$, it is 0.68 and 1.0 for $\theta = 25°C$ and $\theta = 50°C$, respectively. Nevertheless, as the temperature returns to the original value, specimens that previously underwent greater thermal loading will experience more obvious negative pore pressures; for example, when $N = 1$, it is −0.10 and −0.45 for $\theta = 25°C$ and $\theta = 50°C$, respectively. This effect is actually the
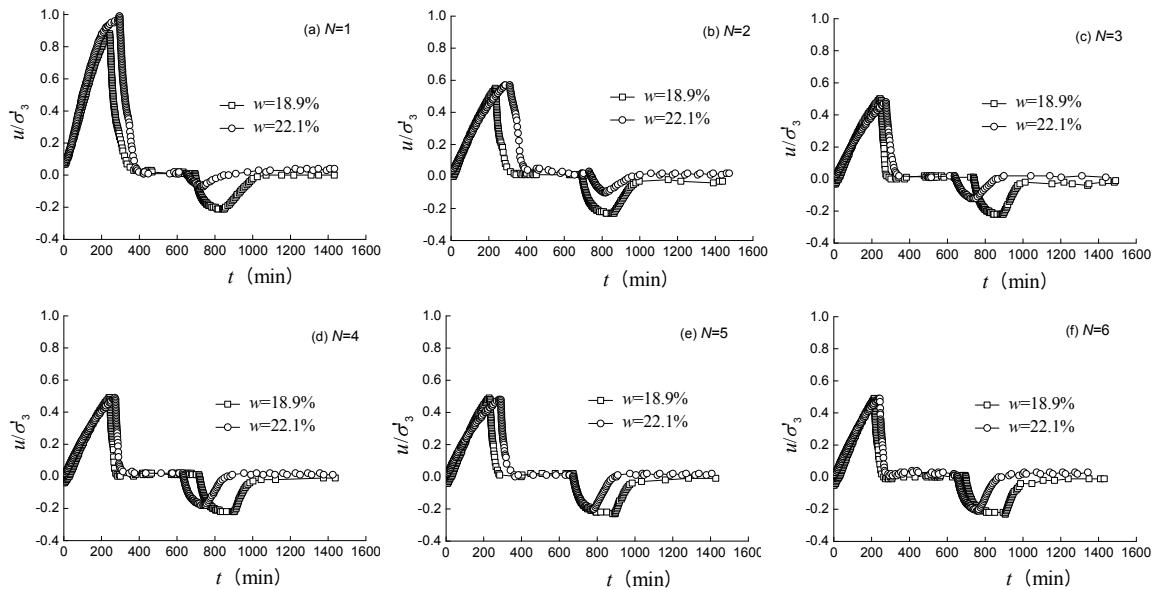

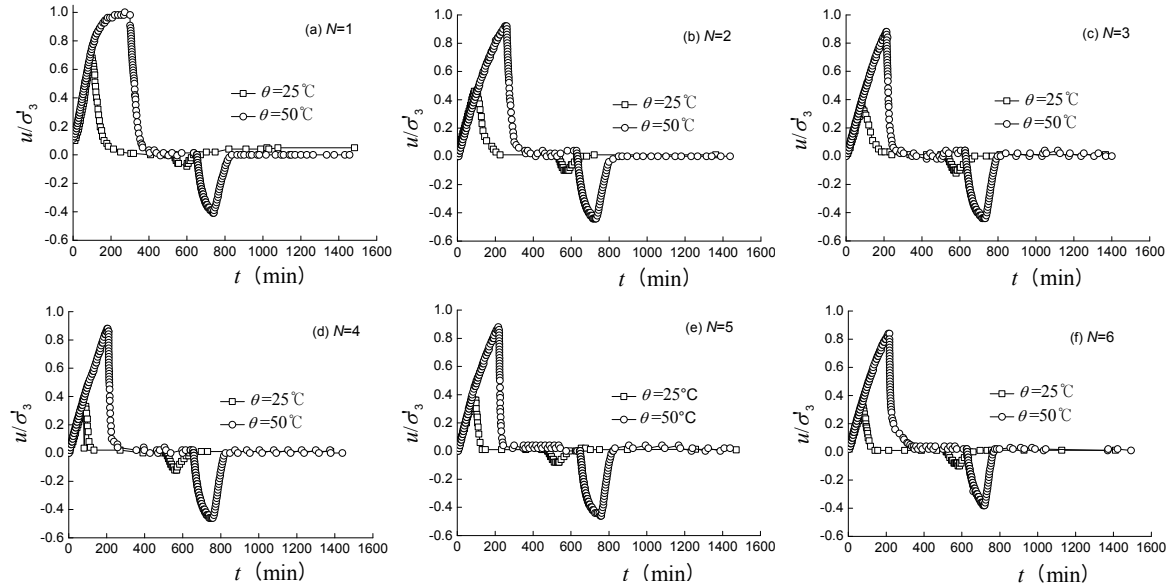Fig. 5 Pore pressure variations for different water contents ($\sigma_3' = 100$ kPa, $\theta = 50°C$)

Fig. 6 Pore pressure variations for different magnitudes of thermal loading ($\sigma_3' = 50$ kPa, $w = 25.1\%$)

result of the thermal loading history on the thermal responses of the saturated soils. It should be noted that the differences regarding pore pressure as a function of the magnitude of thermal loading remain obvious for each cycle. Finally, the residual pore pressures gradually become zero as the result of water absorption.

6. Consolidation volumetric strain variations

6.1 Drained volumetric strains over time

Fig. 7 shows the consolidation volumetric strain evolutions of the specimens with $w = 22.1\%$ during the heating-cooling cycles. Here, the consolidation volumetric strain is defined as $\varepsilon_v = \Delta V/V_0$ expressed as a percentage (%), where V_0 and ΔV are the volume of specimens and expelled water, respectively, both of which are measured at primary temperature T_0. In this study, the so-called consolidation volumetric strain is actually the "drained" thermal volumetric strain measured by the volume of pore water expelled from a specimen under non-isothermal conditions (Cekerevac and Laloui 2004). Fig. 7 shows that $\varepsilon_v = 0$ throughout the undrained heating, indicating the nonexistence of consolidation volume strain; actually, the specimens are expanded because of the expansion of solid grains and pore water. During isothermal consolidation at an elevated temperature (i.e., 75°C), the pore water begins to drain with the dissipation of pore pressure, which leads to a continuous increase of the consolidation volumetric strain, finally reaching a steady state of, e.g., $\varepsilon_v = 2.3\%$ for $N = 1$ ($\sigma_3' = 50$ kPa). During undrained cooling, there is also no change in the consolidation volume strain; actually, the specimens shrink because of the shrinkage of the solid grains and pore water, which can be considered an elastic variation (i.e., being reversible). In other words, the reduction of specimen volume due to the contraction of solid grains and pore water during undrained cooling is the same with the volume expansion during undrained heating. During
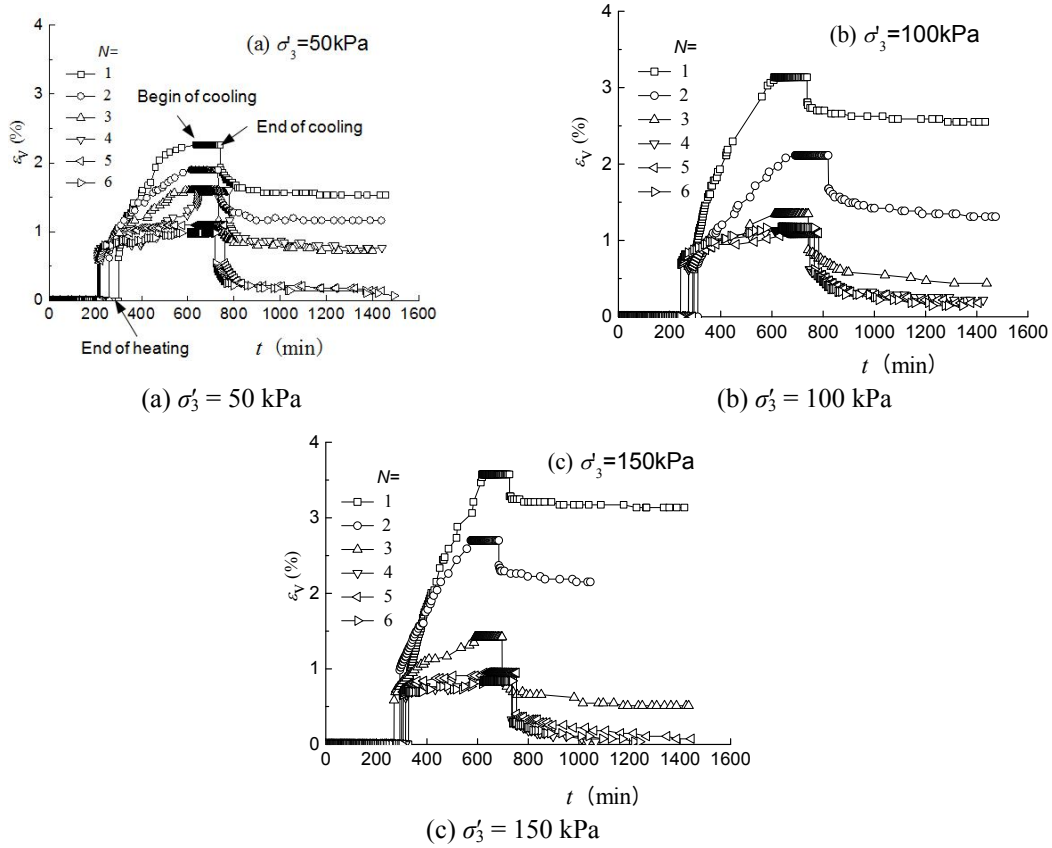
Fig. 7 Consolidation volumetric strain variations during repeated heating-cooling processes
($w = 22.1\%$, $\theta = 50°C$)

isothermal consolidation at a decreased temperature (i.e., 25°C), the saturated specimens begin to increase in volume due to water absorption when the drainage line is opened as compared with the volume of the specimen before water absorption, eventually reaching a steady state of, e.g., $\varepsilon_v = 1.6\%$ for $N = 1$ ($\sigma'_3 = 50$ kPa). On the whole, the specimens tested will show an obvious volume reduction at the completion of a single heating-cooling cycle, indicating the occurrence of an irreversible consolidation deformation.

Table 2 presents the changes of the volumetric strain in each drainage and absorption process. As the number of thermal loading cycles increases, the drainage volumetric strain (being positive, see row 1, 4 and 7 in Table 2) at 75°C tends to decrease. This effect is also true for the volumetric strain after water absorption (see row 2, 5 and 8 in Table 2) at 25°C. Table 2 shows that the volumetric strains for a single heating-cooling cycle tend to become increasingly consistent with each other after several heating-cooling cycles (e.g., $N = 4$) for various confining pressures (i.e., $\sigma'_3 = 50$, 100, and 150 kPa). At this time, the volume of expelled pore water approximately equals the volume of absorbed water (e.g., see the comparison of row 1 and 3 in Table 2 for $\sigma'_3 = 50$ kPa after $N = 4$). Eventually, the volume deformation of the specimens will be completely reversible (i.e., elastic state) from an irreversible state with the further increase of heating-cooling cycles, which can also be verified by the evolutions of pore pressure (see Fig. 4).

Table 2 Volumetric strains under repeated thermal loading

Row	σ_3' (kPa)	T (°C)	Volumetric strain for each cycle ε_v (%)						Final volumetric strain (%)
			1	2	3	4	5	6	
1		75	+2.3	+1.9	+1.6	+1.1	+1.1	+1.0	
2	50	25	1.6	1.2	0.8	0.2	0.1	0.1	3.9
3		Water absorption	−0.7	−0.7	−0.8	−0.9	−1.0	−0.9	
4		75	+3.2	+2.1	+1.4	+1.1	+1.1	+1.1	
5	100	25	2.6	1.3	0.6	0.2	0.2	0.1	5.1
6		Water absorption	−0.6	−0.8	−0.8	−0.9	−0.9	−1.0	
7		75	+3.6	+2.7	+1.4	+1.0	+0.9	+0.8	
8	150	25	3.2	2.1	0.5	0.1	0.1	0.1	6.0
9		Water absorption	−0.4	−0.6	−0.9	−0.9	−0.8	−0.7	

* Note: The plus sign "+" denotes drainage; the minus sign "−" denotes absorption

Table 2 also shows that, with increasing confining pressure, the consolidation volumetric strain during isothermal consolidation at an elevated temperature (see row 1, 4 and 7) or decreased temperature (see row 2, 5 and 8) has an increasing tendency for the first few cycles (e.g., $N = 1, 2$), but it tends to be similar for the last few cycles (e.g., $N = 4, 5, 6$). The physical nature of this phenomenon is consistent with the evolutions of pore pressure presented in section 5.1. In addition, the volumetric deformations at higher confining pressures are higher with respect to the cases with lower confining pressures for the first two cycles. The reason is that, when undrained heating, the specimens undergoing greater consolidation pressures will generate higher pore pressure (i.e., $u =$ 50.0, 97.0, and 127.5 kPa for $\sigma_3' =$ 50, 100, and 150 kPa when $N = 1$; see Fig. 4) and hence have greater thermal consolidation deformations. However, this effect becomes less significant with the increase of heating-cooling cycles due to reversibility. The differences between drainage and absorption volumetric strains are not significant at all times. For example, when $N = 4$, the difference is only 0.2%, 0.2% and 0.1% for $\sigma_3' =$ 50 kPa, 100 kPa and 150 kPa, respectively. The drainage or absorption volumetric strains are mainly determined by temperature variations (being a reversible variation process) and are almost independent of the confining pressures. The final consolidation volumetric strains induced by six heating-cooling cycles are 3.9%, 5.1% and 6.0%, respectively.

6.2 Effects of water content on consolidation volumetric strains

Fig. 8 shows the effects of water content on the consolidation volumetric strains when a confining pressure of 100 kPa is applied. Obviously, the consolidation volumetric strains during isothermal consolidation at an elevated temperature increase with the increase of water content for the first two cycles, but they tend to be similar for the last three cycles. For example, when $N = 1$, the consolidation volumetric strain is 2.7% and 3.2% for $w = 18.9\%$ and 22.1%, respectively, with the difference being 0.5%; when $N = 6$, it is 1.0% and 1.1% for $w = 18.9\%$ and 22.1%, respectively, with the difference being negligible (0.1%). Actually, the specimens with different water contents after an initial consolidation process and several heating-cooling cycles will take on a so-called aging effect, which means that the soil will show an obvious over-consolidated state, gradually
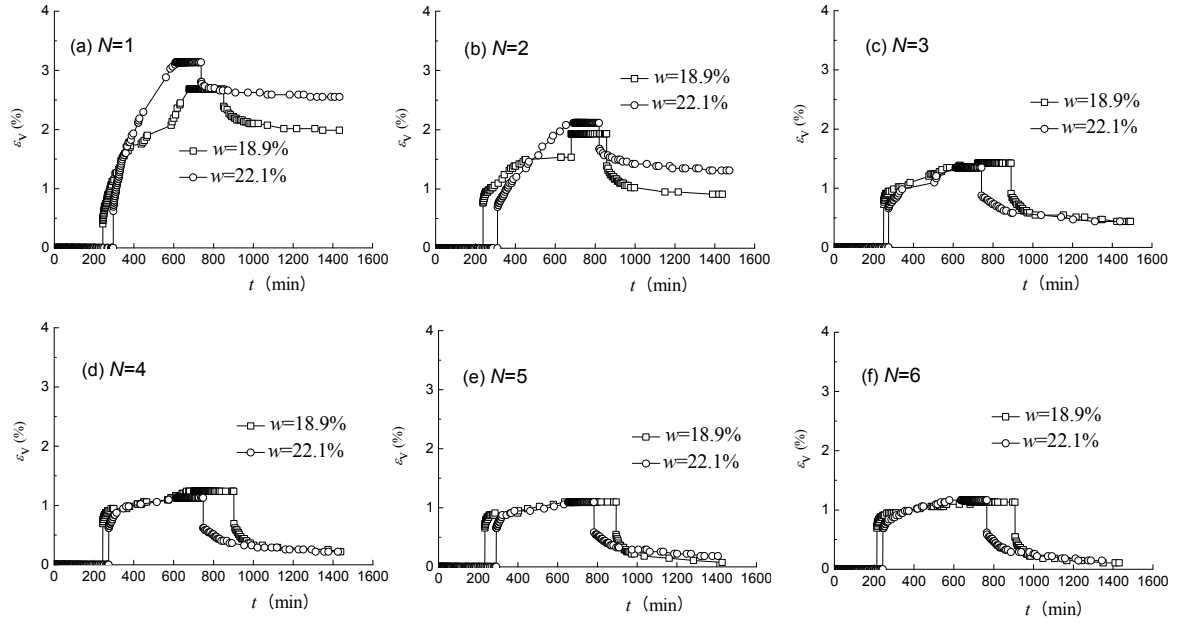
Fig. 8 Consolidation volumetric strain variations for different water contents ($\sigma_3' = 100$ kPa, $\theta = 50°$C)
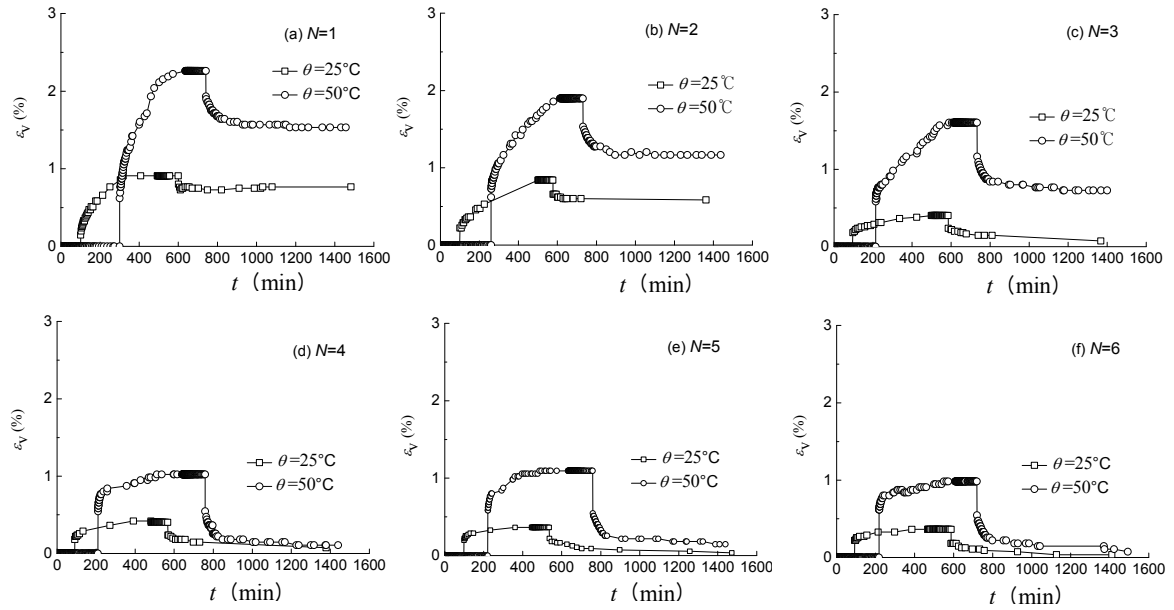

Fig. 9 Consolidation volumetric strain variations for different magnitudes of thermal loading
($\sigma_3' = 50$ kPa, $w = 25.1\%$)

revealing a reversible process. At this time, the volumetric strain variation is mainly determined by the temperature variation and becomes less and less significant cycle after cycle.

6.3 Effects of the magnitude of thermal loading on the consolidation volumetric strains

Fig. 9 shows the effects of the magnitude of thermal loading on the consolidation volumetric strains when w = 25.1% when a confining pressure of 50 kPa is applied. Clearly, the specimens previously subjected to a thermal loading of 50°C will experience a more dramatic consolidation deformation than that of 25°C. With increasing magnitude of thermal loading, the drainage and absorption volumetric strain increases dramatically, as shown in Fig. 9. For instance, when θ = 25°C, the drainage volumetric strain at 75°C and the volumetric strain after water absorption at a decreased temperature (i.e., 25°C) are 0.9% and 0.8% for N = 1, respectively, with the difference (i.e., absorption volumetric strain) being 0.1%; when θ = 50°C, they are 2.3% and 1.5% for N = 1, respectively, with the difference being 0.8%. This result also indicates that after a single heating-cooling cycle, the final volumetric strain increases with the increase of the magnitudes of thermal loading.

7. Conclusions

The salient conclusions drawn from this study are as follows:

(1) Both the maximum normalized and normalized residual pore pressures (after the isothermal consolidation) show a decreasing tendency with the increase of the confining pressure.

(2) During undrained heating, the maximum normalized pore pressure is dramatically increased with the increase of the magnitudes of thermal loading; during the subsequent isothermal consolidation, the normalized residual pore pressures show a slightly increasing tendency. Nevertheless, as the temperature returns to the original value, the specimens that previously underwent greater thermal loading will show more obvious negative pore pressures, indicating an inherent effect of the heating history on the thermal responses.

(3) With the increase of the cyclic numbers of the thermal loading, the pore pressures show a degrading trend, which seems to be more evident under higher confining pressures. More specifically, every time the specimens are heated to the given temperature, the maximum normalized pore pressure will decrease slightly; and every time the temperature returns to the original value under the undrained condition, the minimum normalized pore pressure will decrease slightly, which indicates that the specimens will gradually show an over-consolidated state with repeated heating-cooling cycles.

(4) The maximum normalized pore pressure becomes slightly higher with the increase of water content during undrained heating. However, the difference regarding pore pressure as the function of water content is evident for the first two cycles and then vanishes gradually with the increase of the number of thermal loading cycles.

(5) The drainage volumetric strain is increased greatly with the increase of the water content and magnitudes of thermal loading, while the absorption volumetric strain is also increased at a lower temperature with the increase of the magnitudes of thermal loading. In general, the specimens tested exhibit an obvious volume reduction at the completion of a series of heating-cooling cycles, indicating a notable irreversible thermal consolidation deformation.

Acknowledgments

References

Abuel-Naga, H.M., Bergado, D.T. and Bouazza, A. (2007), "Thermally induced volume change and excess pore water pressure of soft Bangkok clay", *Eng. Geol.*, **89**(1-2), 144-154.

Abuel-Naga, H.M., Bergado, D.T., Bouazza, A. and Pender, M.J. (2009), "Thermal conductivity of soft Bangkok clay from laboratory and field measurements", *Eng. Geol.*, **105**(s3-4), 211-219.

Bai, B. (2006), "Fluctuation responses of saturated porous media subjected to cyclic thermal loading, *Comput. Geotech.*, **33**(4), 396-403.

Bai, B. and Chen, X.X. (2011), "Test apparatus for thermal consolidation of saturated soils and its application", *Chinese J. Geotech. Eng.*, **33**(6), 896-900. [In Chinese]

Bai, B., Guo, L.J. and Han, S. (2014), "Pore pressure and consolidation of saturated silty clay induced by progressively heating/cooling", *Mech. Mater.*, **75**, 84-94.

Baldi, G., Hueckel, T. and Pellegrini, R. (1988), "Thermal volume changes of mineral-water system in low porosity clay soils", *Can. Geotech. J.*, **25**(4), 807-825.

Blond, E., Schmitt, N. and Hild, F. (2003), "Responses of saturated porous media to cyclic thermal loading", *Int. J. Numer. Anal. Methods Geomech.*, **27**(11), 883-904.

Burghignoli, A., Desideri, A. and Miliziano, S. (2000), "A laboratory study on the thermomechanical behaviour of clayey soils", *Can. Geotech. J.*, **37**(4), 764-780.

Cekerevac, C. and Laloui, L. (2004), "Experimental study of thermal effects on the mechanical behavior of a clay", *Int. J. Numer. Anal. Methods Geomech.*, **28**(3), 209-228.

Cheng, X.L. and Wang, J.H. (2016), "An elastoplastic bounding surface model for the cyclic undrained behaviour of saturated soft clays", *Geomech. Eng., Int. J.*, **11**(3), 325-343.

Cui, Y.J., Sultan, N. and Delage, P. (2000), "A thermomechanical model for saturated clays", *Can. Geotech. J.*, **37**(6), 607-620.

Cui, Y.J., Lu, Y.F. and Delage, P. (2005), "Field simulation of in situ water content and temperature changes due to ground-atmospheric interactions", *Geotechnique*, **55**(7), 557-567.

Delage, P., Cui, Y.J. and Tang, A.M. (2010), "Clays in radioactive waste disposal", *J. Rock Mech. Geotech. Eng.*, **2**(2), 111-123.

Delage, P., Sultan, N. and Cui, Y.J. (2012), "On the thermal consolidation of Boom clay", *Can. Geotech. J.*, **37**(2), 343-354.

Francois, B., Laloui, L. and Laurent, C. (2009), "Thermo-hydro-mechanical simulation of ATLAS in situ large scale test in Boom Clay", *Comput. Geotech.*, **36**(4), 626-640.

Ghabezloo, S. and Sulem, J. (2010), "Temperature induced pore fluid pressurization in geomaterials", *Italian Geotech. J.*, **1**, 29-43.

Graham, J., Tanaka, N., Crilly, T. and Alfaro, M. (2001), "Modified Cam-Clay modeling of temperature effects in clays", *Can. Geotech. J.*, **38**(3), 608-621.

Hueckel, T. and Baldi, G. (1990), "Thermoplasticity of saturated clays: experimental constitutive study", *J. Geotech. Eng.*, **116**(12), 1778-1796.

Hüpers, A. and Kopf, A.J. (2009), "The thermal influence on the consolidation state of underthrust sediments from the Nankai margin and its implications for excess pore pressure", *Earth Planet. Sci. Lett.*, **286**(s1-2), 324-332.

Le, T.M., Fatahi, B., Disfani, M. and Khabbaz, H. (2015), "Analyzing consolidation data to obtain elastic viscoplastic parameters of clay", *Geomech. Eng., Int. J.*, **8**(4), 559-594.

Monfared, M., Delage, P., Sulem, J., Mohajerani, M., Tang, A.M. and De Laure, E. (2011), "A new hollow cylinder triaxial cell to study the behavior of geo-materials with low permeability", *Int. J. Rock Mech. Min. Sci.*, **48**(4), 637-649.

Sultan, N., Delage, P. and Cui, Y.J. (2002), "Temperature effects on the volume change behaviour of Boom clay", *Eng. Geol.*, **64**(2-3), 135-145.

Towhata, I., Kuntiwattanaku, P., Seko, I. and Ohishi, K. (1993), "Volume change of clays induced by heating as observed in consolidation tests", *Soils Found.*, **33**(4), 170-183.

Villar, M.V., Gomez-Espina, R. and Lloret, A. (2010), "Experimental investigation into temperature effect on hydro-mechanical behaviours of bentonite", *J. Rock Mech. Geotech. Eng.*, **2**(1), 71-78.

Yavuzturk, C., Ksaibati, K. and Chiasson, A.D. (2005), "Assessment of temperature fluctuations in asphalt pavements due to thermal environmental conditions using a two-dimensional, transient finite-difference approach", *J. Mater. Civil Eng.*, **17**(4), 465-475.

Yilmaz, G. (2011), "The effects of temperature on the characteristics of kaolinite and bentonite", *Sci. Res. Essays*, **6**(9), 1928-1939.

CC